Conditional Lyapunov exponents from time series

K. Pyragas*
Semiconductor Physics Institute, LT-2600 Vilnius, Lithuania
(Received 9 May 1997)

A method for estimating conditional Lyapunov exponents from time series of two unidirectionally coupled chaotic systems is developed. It uses two scalar data sets, one taken from the driving and the other from the response system, and enables one to detect a generalized synchronization in an experiment without recourse to an auxiliary response system. The method is illustrated on coupled maps as well as coupled chaotic flow models. [S1063-651X(97)02311-8]

PACS number(s): 05.45.+b

I. INTRODUCTION

The cooperative behavior of coupled chaotic systems has attracted considerable attention lately. Synchronization effects are observed in many physical and biological processes and they are responsible for the transition to low-dimensional attractors in systems with many degrees of freedom. Synchronization of chaos is often understood as a behavior in which two coupled systems exhibit identical chaotic oscillations [1,2]. We refer to this type of synchronization as an *identical synchronization* (IS).

Recently, the notion of chaotic synchronization has been generalized for coupled nonidentical systems [3,4]. In the case of unidirectionally coupled chaotic systems (master-slave configurations or systems with a skew product structure)

$$\dot{X}=F(X), \tag{1a}$$

$$\dot{Y}=G(Y,X), \tag{1b}$$

generalized synchronization (GS) was taken to occur if there exists a map Φ: $X\rightarrow Y$ that takes the trajectories of the attractor in the driving space $X=\{x_1,x_2,\dots,x_d\}$ into the trajectories of the response space $Y=\{y_1,y_2,\dots,y_r\}$ so that $Y(t)=\Phi(X(t))$ and if this map does not depend upon initial conditions of the response system [4]. When Φ differs from the identity the detection of the GS in an experiment is a difficult task. One way to recognize the GS is to construct an auxiliary response system Y' identical to Y, link it to the driving system X in the same way as Y is linked to X,

$$\dot{Y}'=G(Y',X), \tag{2}$$

and check the existence of the IS between Y and Y' [5]. If such synchronization occurs the asymptotic dynamics of the response system is independent of its initial conditions and is completely determined by the driving system. Geometrically, this implies a collapse of the overall evolution onto a stable synchronization manifold $M=\{(X,Y):\Phi(X)=Y\}$ in the full phase space of two systems $X\oplus Y$ and so leads to a functional relationship between X and Y variables defining the GS [5,6].

Unfortunately, the auxiliary system approach is of limited utility. The method fails for systems whose dynamical equations are not available. Even though the dynamical equations are known (e.g., in electronic circuit experiments [5]), the auxiliary response system can be designed only with finite accuracy; it cannot be an exact copy of the original response system. An alternative approach to detect the GS is to estimate the *conditional Lyapunov exponents* (CLEs) [2] $\lambda_1^R\geqslant\lambda_2^R\geqslant\cdots\geqslant\lambda_r^R$ from observed time series. The CLEs define the stability of both the identity manifold $Y'=Y$ in $X\oplus Y\oplus Y'$ phase space and the synchronized manifold $Y=\Phi(X)$ in $X\oplus Y$ space [5] and are determined by the variational equation of the response system at $\delta X=0$,

$$\delta\dot{Y}=D_YG(Y,X)\,\delta Y, \tag{3}$$

where D_YG denotes the Jacobian matrix with respect to the Y variable. The condition of GS is $\lambda_1^R<0$.

Note that for systems with a skew product structure described by Eq. (1), the CLEs represent a part of the whole Lyapunov spectrum $\lambda_1,\lambda_2,\dots,\lambda_{r+d}$ of this system. The remainder of this spectrum consists of Lyapunov exponents $\lambda_1^D\geqslant\lambda_2^D\geqslant\cdots\geqslant\lambda_d^D$ of the driving system (1a). In other words, to obtain the whole spectrum of Lyapunov exponents of system (1) in usual (descending) order, $\lambda_1\geqslant\lambda_2\geqslant\cdots\geqslant\lambda_{r+d}$, the combined spectrum of the driving Lyapunov exponents and the CLEs $\lambda_1^D,\lambda_2^D,\dots,\lambda_d^D,\lambda_1^R,\lambda_2^R,\dots,\lambda_r^R$ has to be resorted to in order of their numerical size. If the whole spectrum of the Lyapunov exponents is known then one can extract information about the properties of the synchronization manifold.

Depending on the properties of the map Φ, the GS can be subdivided into two types: *weak synchronization* (WS) and *strong synchronization* (SS) [7]. The WS is associated with the continuous C^0 but nonsmooth map Φ so that the synchronization manifold $M=\{(X,Y):\Phi(X)=Y\}$ has a fractal structure and the global dimension d_G of the strange attractor in the whole phase space $X\oplus Y$ is larger than the dimension of the driving attractor d_D in X subspace, $d_G>d_D$. The SS is related to the smooth map Φ with the degree of smoothness C^1 or higher when the response system does not have an

*Electronic address: pyragas@kes0.pfi.lt

effect on the global dimension, i.e., $d_G = d_D$ [8]. This is valid, for example, for the IS, which is a particular case of the SS.

In most cases dimensions d_G and d_D can be estimated from the Kaplan-Yorke conjecture [9]

$$d_G = l_G + \frac{1}{|\lambda_{l_G+1}|} \sum_{l=1}^{l_G} \lambda_l , \tag{4}$$

$$d_D = l_D + \frac{1}{|\lambda_{l_D+1}^D|} \sum_{l=1}^{l_D} \lambda_l^D , \tag{5}$$

where l_G and l_D are the largest integers for which the corresponding sums over l are non-negative. The global Lyapunov dimension is independent of the response system ($d_G = d_D$) at the condition [7] $\lambda_1^R < \lambda_{l_D+1}^D$. If this condition is fulfilled and relations (4) and (5) are valid, we have the SS.

Note that only a finite number of Lyapunov exponents can be reliably determined from data on the attractor [10]. An appropriate cutoff value for the number of exponents is related to the global Lyapunov dimension and is equal to $l_G + 1$. The only exponents that are included in Eq. (4) are fundamentally important to the character of the attractor and their estimation is available from time series. In the case of WS at least a maximal CLE affects the global dimension and hence can be estimated from time series. The condition of strong synchronization $\lambda_1^R < \lambda_{l_D+1}^D$ corresponds to the case when the global dimension d_G does not depend on CLEs. Thus we cannot expect a reliable estimation of CLEs from time series above the threshold of SS. However, the CLEs can be determined just before this threshold and this suffices to estimate characteristic values of control parameters corresponding to the onset of SS.

II. ALGORITHM

Suppose that an experimental system under investigation can be simulated by Eqs. (1). We imagine that the equations are unknown, but two scalar time series x_i and y_i, $i = 1,\ldots,N$, corresponding to the driving and response subsystems, respectively, are available for observation. We assume that the time interval τ between measurements is fixed so that $x_i = x(i\tau)$ and $y_i = y(i\tau)$. Below τ is identified with the delay time of phase-space reconstruction in step (a) of our algorithm. In principle, any choice of τ is acceptable in the limit of an infinite amount of data. For a small amount of data, the choice of τ can be based, for example, on the evaluation of mutual information [11].

Due to the unidirectional coupling the x_i series does not contain any information about the response system, while the y_i series does contain the information about both subsystems. Since the CLEs represent a part of the whole Lyapunov spectrum, one can expect that they can be determined by the standard algorithms [10,12,13] from y_i time series. However, the CLEs may be placed far from the maximal Lyapunov exponent in the whole spectrum ordered in descending fashion, while the standard algorithms give reliable values only for a few largest exponents [10,12,13]. Moreover, there is a nontrivial problem to define which exponents belong to the CLEs and which to the driving system, even though the whole spectrum of the Lyapunov exponents is reliably determined. These problems can be solved in the framework of the algorithm involving information from both scalar time series x_i and y_i. Here we mainly use the ideas of the algorithm proposed by Eckmann *et al.* [13] based on the construction of local linear maps. The mappings with a higher order of Taylor series [10] are beyond our scope. We extend the Eckmann-Kamphorst-Ruelle-Ciliberto (EKRC) algorithm for the case of two time series and adopt it for the direct estimation of the CLEs. The reliability of estimating the maximal CLE by our algorithm is comparable to that of estimating the conventional maximal Lyapunov exponent by the EKRC algorithm. A copy of the computer program implementing this algorithm can be obtained from the author.

To speed up the computation and to bring our consideration closer to a real experimental situation we present the time series x_i and y_i by integer numbers normed to the same maximal value M_0 so that $0 \leqslant x_i \leqslant M_0$ and $0 \leqslant y_i \leqslant M_0$. Typically we take $M_0 = 10\,000$ in accordance with a precision of 10^{-4}. Similarly to the EKRC algorithm, our algorithm involves the following three steps: (a) reconstructing the dynamics by the time-delay method [14] and finding the neighbors of the fiducial trajectory, (b) obtaining the tangent maps by a least-squares fit, and (c) deducing the CLEs from the tangent maps. Now we consider these steps in detail.

(a) We choose different embedding dimensions E_x and E_y for the driving and response systems and define $(E_x + E_y)$-dimensional vectors

$$R_i = \{x_{i-E_x+1},\ldots,x_{i-2},x_i,y_{i-E_y+1},\ldots,y_{i-2},y_i\} \tag{6}$$

for $i = i_0 \equiv \max(E_x,E_y)$, $i_0+1,\ldots,N$, to construct the dynamics of the fiducial trajectory in the whole $X \oplus Y$ phase space. In view of step (b) we have to determine the neighbors of R_i, i.e., the points R_j of the orbit that are contained in a ball of small radius ϵ_i centered at R_i,

$$\|R_j - R_i\| \leqslant \epsilon_i . \tag{7}$$

Here $\| \ \|$ implies the maximal projection of the vector rather than the Euclidean norm. This allows a fast search for the R_j by first sorting the data [13]. Denote by J_i the number of neighbors R_j of R_i within a distance ϵ_i, as determined by Eq. (7). Clearly, J_i depends on ϵ_i. In (b) we discuss the choice of these parameters for every i.

(b) Having embedded our dynamical system, we want to determine the tangent map that describes how the time evolution sends small vectors around $R_i = \{X_i, Y_i\}$ to small vectors around Y_{i+m}. This problem can be considered in the phase space of reduced dimension [13]. Following Ref. [10], we introduce the local dimensions $L_x \leqslant E_x$ and $L_y \leqslant E_y$ that reflect the number of dimensions necessary to capture the geometry of a small neighborhood of the attractor after it has been successfully embedded (i.e., the time-delay representation is diffeomorphic to the original attractor). Dimensions L_x and L_y are used for constructing the local maps and correspond to the number of Lyapunov exponents of the driving system and CLEs, respectively, produced by algorithm. The transition from embedding dimensions to local dimensions is performed similarly to that in Ref. [13]. We drop the intermediate components in Eq. (6) and define the L_x-dimensional X_i and L_y-dimensional Y_i vectors as

$$X_i=(x_{i-E_x+1},\ldots,x_{i-m},x_i)^T, \tag{8a}$$

$$Y_i=(y_{i-E_y+1},\ldots,y_{i-m},y_i)^T. \tag{8b}$$

The dimensions $L_x\leqslant E_x$ and $L_y\leqslant E_y$ are determined by equalities $E_x=(L_x-1)m+1$ and $E_y=(L_y-1)m+1$, which we assume to hold for some integer $m\geqslant 1$. The case $m=1$ corresponds to $L_x=E_x$, $L_y=E_y$. When $m>1$ the dimension of the tangent map is reduced with respect to the embedding dimension and this can help to avoid the spurious Lyapunov exponents [13].

The tangent map is defined by two matrices A_i and B_i, which are obtained by looking for neighbors R_j of R_i and imposing

$$A_i(X_j-X_i)+B_i(Y_j-Y_i)\approx Y_{j+m}-Y_{i+m}. \tag{9}$$

A_i is the rectangular $L_y\times L_x$ matrix and B_i is the square $L_y\times L_y$ matrix, which in view of Eqs. (8) and (9) have the form

$$A_i=\begin{pmatrix} 0 & 0 & \cdots & 0\\ 0 & 0 & \cdots & 0\\ \vdots & \vdots & \vdots & \vdots\\ 0 & 0 & \cdots & 0\\ a_1^i & a_2^i & \cdots & a_{L_y}^i \end{pmatrix},$$

$$B_i=\begin{pmatrix} 0 & 1 & 0 & \cdots & 0\\ 0 & 0 & 1 & \cdots & 0\\ \vdots & \vdots & \vdots & & \vdots\\ 0 & 0 & 0 & \cdots & 1\\ b_1^i & b_2^i & b_3^i & \cdots & b_{L_y}^i \end{pmatrix}.$$

Matrix A_i contains L_x unknown elements a_k^i, $k=1,2,\ldots,L_x$, and matrix B_i contains L_y unknowns b_k^i, $k=1,2,\ldots,L_y$. These L_x+L_y unknowns are obtained by a least-squares fit

$$\min_{a_k^i,b_k^i}\frac{1}{J_i}\sum_{j=1}^{J_i}\|A_i(X_j-X_i)+B_i(Y_j-Y_i)-(Y_{j+m}-Y_{i+m})\|_{Euc}^2,$$

where $\|\ \|_{Euc}^2$ denotes the square of the Euclidean norm of the vector. This problem reduces to a set of L_x+L_y linear equations with respect to L_x+L_y unknowns a_k^i,b_k^i, which we solve by the LU decomposition algorithm [15]. Obviously, this algorithm fails if the number of neighbors R_j of the fiducial point R_i is less than the number of unknowns, $J_i<L_x+L_y$. To avoid this problem the radius ϵ_i has to be chosen to be sufficiently large. For the specific examples discussed below we have selected ϵ_i and J_i as follows. Count the number of neighbors J_i of R_i corresponding to increasing values of ϵ_i from a preselected sequence of possible values and stop when J_i exceeds for the first time $J_{\min}=2(L_x+L_y)$. To speed up the calculations we also stop the search for the neighbors when for given ϵ_i the number of neighbors exceeds some maximal value $J_{\max}=40$. Thus, for every i, J_i is in the interval $[J_{\min},J_{\max}]$.

(c) Step (b) gives matrices A_i and B_i of the tangent map, which represent the reconstructed Jacobians D_xG and D_yG of Eq. (1b) with respect to X and Y variables, respectively. The CLEs are determined by the product of the matrices $B_{i_0}B_{i_0+m}B_{i_0+2m}\cdots$. To extract the CLEs from this product we use the QR decomposition technique [13,15]. The method recursively defines an orthogonal matrix Q_l and an upper triangular matrix R_l, $l=0,1,\ldots,L-1$, via $B_{i_0+lm}Q_l=Q_{l+1}R_{l+1}$, where Q_0 is the unit matrix. The CLEs are given by

$$\lambda_n^R m=\frac{1}{\tau L}\sum_{l=0}^{L-1}\ln(Q_l)_{nn},$$

where $K<(N-i_0)/m$ is the available number of matrices and $(Q_l)_{nn}$ is the diagonal element of the matrix Q_l. Note that in final step we do not require a knowledge of the matrix A_i. However, the use of this matrix in step (b) is necessary in order to determine correctly the tangent map (9) and hence the matrix B_i defining the CLEs.

Now we illustrate our algorithm with two specific examples.

III. EXAMPLES

A. Coupled Hénon maps

The first example represents two identical unidirectionally coupled Hénon [16] maps

$$\begin{pmatrix} x_1(i+1)\\ x_2(i+1)\end{pmatrix}=\begin{pmatrix} f[x_1(i),x_2(i)]\\ bx_1(i)\end{pmatrix}, \tag{10a}$$

$$\begin{pmatrix} y_1(i+1)\\ y_2(i+1)\end{pmatrix}=\begin{pmatrix} (1-k)f[y_1(i),y_2(i)]+kf[x_1(i),x_2(i)]\\ by_1(i)\end{pmatrix}, \tag{10b}$$

where $f[x_1,x_2]=1-ax_1^2+x_2$, $a=1.4$, $b=0.3$, and k is the control parameter defining the coupling strength. At any k, this system has an invariant manifold $Y=X$ and hence admits the IS, which in this case is equivalent to the SS. The IS appears when the manifold $Y=X$ becomes stable. This happens when k exceeds some threshold $k>k_3\approx 0.34$ so that the transverse Lyapunov exponents of the manifold $Y=X$ become negative. Before reaching this threshold, the system exhibits the GS in the form of WS. This is observed in the interval of parameter $k\in[k_1,k_2]$, with $k_1\approx 0.16$ and $k_2\approx 0.20$. Here the maximal CLE is negative, while the maximal transverse Lyapunov exponent of the identity manifold $Y=X$ is positive. This means that systems Y and Y' [here by Y' we imply the auxiliary response system constructed in accordance with Eq. (10b)] are synchronized in the sense of IS and there is no IS between X and Y.

To test the algorithm two scalar time series $x_1(i)$ and $y_1(i)$ were treated as experimental data. The results presented in Table I correspond to a fixed value $k=0.1$ and different values of local dimensions L_x and L_y. For comparison, we calculated the correct values of CLEs $\lambda_1^R\approx 0.227$ and

TABLE I. CLEs for coupled Hénon maps at $k=0.1$ computed from $N=50\,000$ data points evaluated with the sampling time $\tau=1$. We vary the local dimensions L_x and L_y at fixed $m=1$ so that they coincide with the embedding dimensions, $E_x=L_x$ and $E_y=L_y$. The correct values of CLEs calculated directly from Eqs. (10) are $\lambda_1^R\approx 0.227$, $\lambda_2^R\approx -1.537$. For $L_y>2$, the algorithm gives L_y-2 spurious CLEs in parallel with two valid CLEs. The values corresponding to the valid CLEs are underlined.

L_y	L_x	λ_1^R	λ_2^R	λ_3^R	λ_4^R
2	2	$\underline{0.228}$	$\underline{-1.408}$		
2	3	$\underline{0.224}$	$\underline{-1.411}$		
2	4	$\underline{0.219}$	$\underline{-1.402}$		
3	2	0.462	$\underline{0.203}$	$\underline{-1.558}$	
3	3	0.459	$\underline{0.186}$	$\underline{-1.547}$	
3	4	0.489	$\underline{0.178}$	$\underline{-1.546}$	
4	2	0.530	$\underline{0.206}$	-0.962	$\underline{-1.629}$
4	3	0.512	$\underline{0.189}$	-0.863	$\underline{-1.612}$
4	4	0.536	$\underline{0.191}$	-0.786	$\underline{-1.613}$

$\lambda_2^R\approx -1.537$ ($k=0.1$) using Eqs. (10). For any $L_x\geqslant 2$ and $L_y\geqslant 2$, the algorithm gives two CLEs close to these correct values. If L_y is chosen correctly [i.e., equal to the dimension of the response system (10b) $L_y=r=2$] we obtain the right number of CLEs whose values weakly depend on L_x provided $L_x\geqslant 2$. For $L_y>2$, the algorithm gives spurious CLEs in parallel with valid CLEs.

One way of identifying spurious exponents is to analyze the influence of external noise [10]. This is illustrated in Fig. 1. We have added Gaussian white noise to the data points with the standard deviation σ. In Fig. 1(a) we have used $L_x=L_y=2$, while in Fig. 1(b) we used $L_x=L_y=3$, which gives

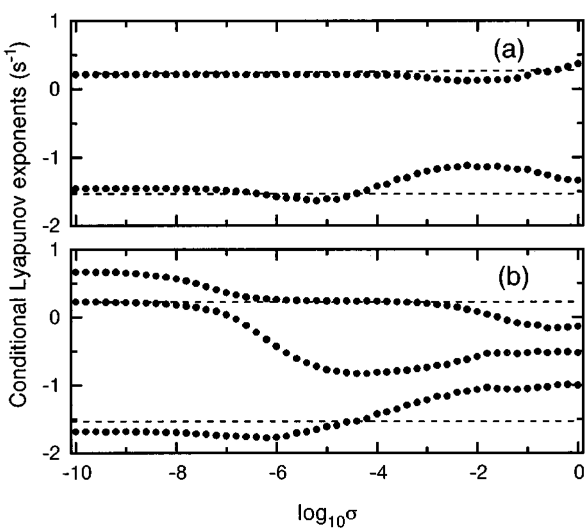

FIG. 1. Effect of external noise on the determination of CLEs for coupled Hénon maps at the same values of parameters as in Table I. σ is the standard deviation of noise added to the data. Local dimensions are (a) $L_x=L_y=2$ and (b) $L_x=L_y=3$. The spurious exponent wanders from about $+0.7$ to nearly -0.9 as the noise level is increased. The exponents do not cross each other, but switch roles as they become close. The correct values of the CLEs are shown by dotted lines.

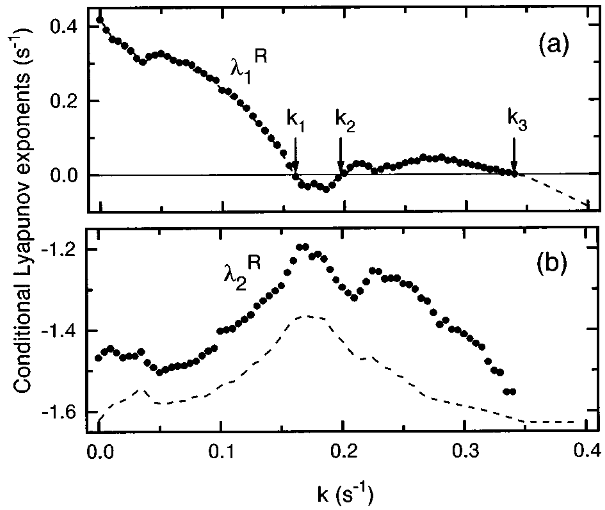

FIG. 2. Dependence of CLEs on coupling strength for coupled Hénon maps at $m=1$, $L_x=L_y=2$. The points correspond to the values of CLEs estimated from time series and the dotted lines show the correct values of CLEs calculated directly from Eqs. (10). The interval $k_1<k<k_2$ corresponds to the WS. At $k>k_3$ systems (10a) and (10b) exhibit identical behavior corresponding to the SS.

one spurious CLE. The spurious CLE in Fig. 1(b) drops rapidly as the added noise is increased, going from $+0.7$ down to -0.9.

Figure 2 shows a correlation between the dependence of CLEs on the coupling strength k estimated from time series with that calculated directly from Eqs. (10). Good agreement, especially for the maximal CLE, is observed for $k<k_3$. For $k>k_3$, we have the SS with identical time series $y_1(i)=x_1(i)$ and the algorithm fails. This is in agreement with the general prediction that CLEs cannot be reliably estimated from time series in the domain of SS. However, the algorithm gives the correct values of the maximal CLE in the immediate vicinity of the threshold $k\lesssim k_3$.

B. Coupled Rössler and Lorenz systems

As a second example we choose the model considered in Ref. [7], which illustrates the GS in essentially different time-continuous systems. It represents unidirectionally coupled Rössler [17] and Lorenz [18] equations

$$\frac{d}{dt}\begin{pmatrix} x_1\\ x_2\\ x_3\end{pmatrix}=\alpha\begin{pmatrix} -x_2-x_3\\ x_1+0.2x_2\\ 0.2+x_1x_3x_1-5.7x_3\end{pmatrix}, \tag{11a}$$

$$\frac{d}{dt}\begin{pmatrix} y_1\\ y_2\\ y_3\end{pmatrix}=\begin{pmatrix} 10(-y_1+y_2)\\ 28y_1-y_2-y_1y_3\\ y_1y_2-8/3y_3\end{pmatrix}+k\begin{pmatrix} 0\\ x_2\\ 0\end{pmatrix}. \tag{11b}$$

Here Eqs. (11a) and (11b) correspond to the Rössler (driving) and the Lorenz (response) system, respectively. The multiplier $\alpha=6$ is introduced to control the time scale of the driving system. The last term in Eq. (11b) describes the coupling, where k is the coupling strength. Despite the lack of any symmetry admitting the IS, this system exhibits the GS [7].

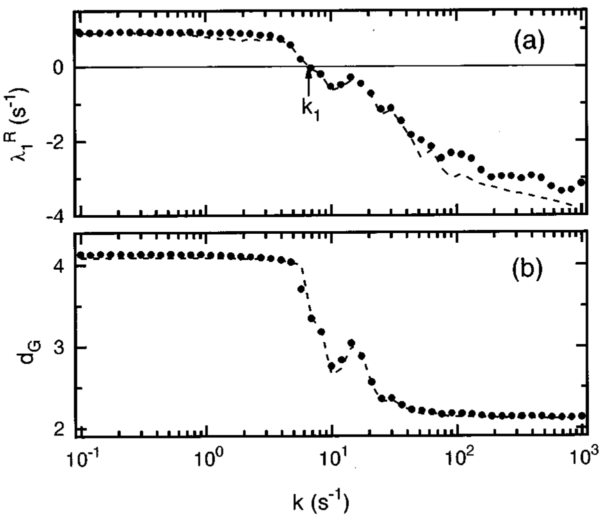

FIG. 3. (a) Maximal CLE λ_1^R and (b) global Lyapunov dimension d_G as functions of the coupling strength k for coupled Rössler and Lorenz systems at $N=50\,000$, $\tau=0.15$ for $k\leqslant 10$, and $\tau=0.03$ for $k>10$. The local dimensions $L_x=L_y=3$ and $m=1$. To estimate d_G one needs a knowledge of the Lyapunov exponents of the driving system, $\lambda_1^D\approx 0.41$, $\lambda_2^D\approx 0.00$, and $\lambda_3^D\approx -37.66$. We evaluated them by a standard EKRC algorithm from $x_1(t)$ time series. The threshold of GS $k_1\approx 6.66$ corresponds to $\lambda_1^R(k_1)=0$. The global dimension d_G saturates to the value approximately equal to the driving dimension $d_D=2+\lambda_1^D/|\lambda_3^D|\approx 2.01$ at $k>40$. In this domain, the synchronization manifold is almost smooth. For comparison, the correct characteristics $\lambda_1^R(k)$ and $d_G(k)$ determined directly from Eqs. (11) are shown by dotted lines.

When testing the algorithm, the variables $x_1(t)$ and $y_1(t)$ were treated as experimentally available outputs. In Figs. 3(a) and 3(b), the calculated maximal CLE and the global Lyapunov dimension, respectively, are shown as functions of coupling strength k. For comparison, the same characteristics determined directly from Eqs. (11) are presented. Good agreement of corresponding characteristics is observed in a large interval of coupling strengths. These results allow us to estimate both the threshold of GS and the smoothness of the synchronization manifold. The threshold of GS is obtained from $\lambda_1^R(k_1)=0$ and is approximately equal to $k_1\approx 6.66$. In the case of the driving system presented by a three-dimensional flow the condition of SS becomes $\lambda_1^R(k)<\lambda_3^D$. For the system of equations (11a), we have $\lambda_1^D\approx 0.41$, $\lambda_2^D\approx 0.00$, and $\lambda_3^D\approx -37.66$ and the driving Lyapunov dimension is equal to $d_D=2+\lambda_1^D/|\lambda_3^D|\approx 2.01$. Because of the large negative value of λ_3^D the condition $\lambda_1^R(k)<\lambda_3^D$ is not achieved even for very large $k\approx 1000$. Thus we have the WS for all $k>k_1$ and the algorithm of estimating CLEs from time series works well in the whole considered interval of k. Although the rigorous criterion of WS $d_G(k)>d_D$ is fulfilled for all $k>k_1$, the global dimension goes down to the value approximately equal to the driving dimension at $k\gtrsim 40$. Here the global dimension is $d_G(k)=2+\lambda_1^D/|\lambda_1^R(k)|$ and since $\lambda_1^D/|\lambda_3^D|\ll 1$ and $\lambda_1^D/|\lambda_1^R|\ll 1$, we have $d_G(k)\approx d_D\approx 2$. Therefore, one can conclude that the synchronization manifold is almost smooth at $k\gtrsim 40$. This conclusion is confirmed in Ref. [7] by calculating the mean local thickness of the synchronization manifold. The region $k\gtrsim 40$ can be interpreted as a domain of not fully developed SS.

In addition to the examples presented we used the algorithm for real experimental data taken from coupled electronic chaos oscillators and successfully obtained the domain of GS as well as properties of synchronization manifold [19].

IV. CONCLUSION

An algorithm for estimating conditional Lyapunov exponents from two scalar time series, one taken from the driving X and the other from the response Y, system, is suggested. This analysis of experimental data enables one to detect the generalized synchronization in unidirectionally coupled chaotic systems. As a consequence, one can predict (without recourse to an experimental auxiliary response system) whether an identical copy Y' of the response system connected to the driving system X will exhibit a behavior identical to the original response system Y. In the domain of generalized synchronization, one can estimate the smoothness of the synchronization manifold. This estimate is based on a comparison of the global Lyapunov dimension with the dimension of the driving attractor.

[1] H. Fujisaka and T. Yamada, Prog. Theor. Phys. **69**, 32 (1983).
[2] L. M. Pecora and T. L. Carroll, Phys. Rev. Lett. **64**, 821 (1990).
[3] V. S. Afraimovich, N. N. Verichev, and M. I. Rabinovich, Radiophys. Quantum Electron. **29**, 795 (1986).
[4] N. F. Rulkov, M. M. Sushchik, L. S. Tsimring, and H. D. I. Abarbanel, Phys. Rev. E **51**, 980 (1995).
[5] H. D. I. Abarbanel, N. F. Rulkov, and M. M. Sushchik, Phys. Rev. E **53**, 4528 (1996).
[6] L. Kocarev and U. Parlitz, Phys. Rev. Lett. **76**, 1816 (1996).
[7] K. Pyragas, Phys. Rev. E **54**, R4508 (1996).
[8] T. Sauer and J. A. Yorke, Ergodic Theory Dyn. Syst. (to be published). The authors provide a theorem that shows that the continuously differentiable (C^1) maps preserve the dimension of strange attractors.
[9] J. L. Kaplan and J. A. Yorke, in *Functional Differential Equations and Approximation of Fixed Points*, edited by H.-O. Peitgen and H.-O. Walther, Lecture Notes in Mathematics Vol. 730 (Springer-Verlag, Berlin, 1979), p. 204; Phys. Rev. A **34**, 4971 (1986).
[10] P. Bryant, R. Brown, and H. D. I. Abarbanel, Phys. Rev. Lett. **65**, 1523 (1990); R. Brown, P. Bryant, and H. D. I. Abarbanel, Phys. Rev. A **43**, 2787 (1991).
[11] A. M. Fraser and H. L. Swinney, Phys. Rev. A **33**, 1134 (1986).
[12] A. Wolf, J. B. Swift, H. L. Swinney, and J. A. Vastano, Physica D **16**, 285 (1985).
[13] J.-P. Eckmann, S. O. Kamphorst, D. Ruelle, and S. Ciliberto, Phys. Rev. A **34**, 4971 (1986).
[14] N. H. Packard, J. P. Crutchfield, J. D. Farmer, and R. S. Shaw,

Phys. Rev. Lett. **45**, 712 (1980).
[15] W. H. Press, S. A. Teukolsky, W. T. Vetterling, and B. P. Flannery, *Numerical Recipes in C. The Art of Scientific Computing*, 2nd ed. (Cambridge University Press, Cambridge, 1994).
[16] M. Hénon, Commun. Math. Phys. **50**, 69 (1976).
[17] O. E. Rössler, Phys. Lett. **57A**, 397 (1976).
[18] E. N. Lorenz, J. Atmos. Sci. **20**, 130 (1963).
[19] A. Kittel, J. Parisi, and K. Pyragas, Physica D (to be published).